Korean J. Chem. Eng., 25(6), 1524-1531 (2008)

Porosity distribution in highly compressible cake: Experimental and theoretical verification of the dense skin

Sung Sam Yim and Yun Min Song†

Department of Environmental Engineering, Inha University, Incheon 402-751, Korea
(*Received 23 February 2008 • accepted 24 June 2008*)

Abstract−The rate of filtration and the water content of cake are influenced by the existence of a dense skin in a highly compressible cake. The phenomenon of the dense skin has been rarely studied, and its existence has not been verified experimentally. In this study, the porosity variation in a very compressible cake is measured by using a new experimental apparatus, and with this the existence of dense skin has been established experimentally. 'Unified theory on solid-liquid separation', a recently developed theory, is utilized for calculating the porosity variation in a very compressible cake.

Key words: Cake Filtration, Dense Skin, Very Compressible Cake, Porosity, Porosity Distribution

INTRODUCTION

Carman [1] insisted that "a compressible cake is 'drier,' i.e., less porous, at the cloth than at the face", and it is "a phenomenon often very pronounced in very gelatinous cakes." However, this phenomenon has neither been analyzed theoretically nor verified experimentally.

Tiller and Green [2] calculated the porosity distribution in a cake, and they found that the porosity of a very compressible cake has a peculiar distribution. That is, "a thin skin of dry, resistant material is formed next to the media during filtration" by the sharp decrease of porosity next to the filter media. This thin skin was named "dense skin." They insisted that "most of the hydraulic pressure drop is located within that narrow region." Calculations for various filtration pressures showed that the resistance of the thin layer (dense skin) increases sharply at high filtration pressure.

For filtrations with a normally compressible cake, the filtration rate is in proportion to the filtration pressure, and the water content decreases due to the high pressure. The dense skin in a highly compressible cake prevents an increase of the filtration rate and a decrease of cake water content by high pressure [3]. Nevertheless, high filtration pressure is still applied with the aim of attaining a fast flow rate or a high solid content cake, but it is not adequate for highly compressible cake filtration.

At present, cake filtration is widely and extensively performed for natural coagulated materials such as digested activated sludge formed at wastewater plants, as well as for artificially coagulated materials. The coagulated materials form highly compressible cakes. Accordingly, study on such cakes has significant implications. The present authors believe that experimental verification of the existence of a 'dense skin' in the context of studying the filtration characteristics of highly compressible cake is among the most important topics in this field.

The available experimental methods for measuring the porosity distribution are as follows. Measuring the electrical conductivities in a cake and transforming these into porosities have been attempted by Rietema [4] and Shirato et al. [5]. Measurement of the liquid pressure at various depths in cake [6] can give the solid compressive pressures which could easily be translated into porosities.

Hutto [7] filtered a fixed amount of suspension and then filtered a small amount of colored suspension of the same character. Continuing this process, a cake with colored bands was obtained and the variation of the porosity with depth was measured.

These experimental methods can be applied to the filtration of suspensions composed of particles, which form normally compressible cakes. For the filtration of sedimented floc, which forms a highly compressible cake, neither of these methods can be applied.

In this study, cake formed by floc filtration was sliced in 1 mm or 2 mm sections and then dried. The weights of the sections were then measured to determine the porosities.

On the basis of the porosity distribution in a very compressible cake, the existence of the dense skin will be proved experimentally. We also investigate the characteristics of the dense skin theoretically using the "unified theory in solid-liquid separation."

THEORETICAL ANALYSIS

1. Calculation of Porosity Distribution in a Cake

1-1. Equation for Porosity Distribution

Tiller [8] proposed a mathematical method for calculating the porosity distribution in a cake. When pressure dp_l [Pa] is applied on a very thin cake dW [kg/m^2], the flow rate can be described as Eq. (1). This concept originates from Darcy's equation [9].

$$v_o = \frac{dp_l}{\mu\alpha dW} \tag{1}$$

Here, v_o is the rate of flow of the filtrate in an empty vessel [m/s], p_l is the pressure on the liquid [Pa], μ is the viscosity of the filtrate, α is the specific resistance of the cake [m/kg], and W [kg/m^2] is the mass of dry cake per filtration area [m^2]. This equation means that the increment of pressure p_l results in a proportional increase of the filtrate flow rate v_o through dW.

Denoting the liquid pressure at a certain point in the cake as p_l,

†To whom correspondence should be addressed.
E-mail: bluepobe@hanmail.net

and the solid compressive pressure at the same height as p_s, the relation between the two pressures is as below:

$$p_l+p_s=\Delta p \tag{2}$$

This means that the sum of liquid pressure p_l and solid compressive pressure p_s at any point in the cake is Δp, which is the total applied pressure to the cake. As the value of Δp does not change during constant pressure filtration, Eq. (3) can be obtained by integrating Eq. (2).

$$dp_l+dp_s=0 \tag{3}$$

When Eq. (3) is introduced into Eq. (1), we can obtain:

$$\frac{dp_l}{dW}=-\frac{dp_s}{dW}=\mu\alpha v_o \tag{4}$$

If the cake thickness under consideration is dx [m], the cake volume can be determined by multiplying the filtration area A [m^2], i.e., Adx [m^3]. Here, x [m] is the distance from the surface of the filter medium to a certain position of the cake, and L [m] is the total cake thickness.

The cake porosity is normally denoted as ε [-]. The volume of particles in the cake is $(1-\varepsilon)$Adx [m^3]. When the density of particles, ρ_s [kg/m^3], is introduced, the mass of total particles is given as $\rho_s(1-\varepsilon)$Adx [kg]. Finally, the mass of particles per unit filtration area is expressed as Eq. (5).

$$dW=\rho_s(1-\varepsilon)dx \tag{5}$$

Introducing Eq. (5) to Eq. (4) and rearranging yields

$$-\frac{dp_s}{dx}=\mu\rho_s(1-\varepsilon)\alpha v_o \tag{6}$$

As the values of $(1-\varepsilon)$ and α are directly proportional to the solid compressive pressure p_s, Eq. (6) can be changed to the form of Eq. (7).

$$-\frac{dp_s}{\alpha(1-\varepsilon)}=\mu\rho_s v_o dx \tag{7}$$

Integrating Eq. (7) for the whole cake gives

$$-\int_{\Delta p}^{0}\frac{dp_s}{\alpha(1-\varepsilon)}=\mu\rho_s v_o\int_0^L dx \tag{8}$$

In Table 1, all the boundary conditions applicable to the cake filtration are expressed.

In this study, the pressure drop through the filter cake is defined as Δp. Practically, the total pressure drop for filtration requires a small additional pressure drop in order to pass the filter medium. However, we employ a simplified definition for convenience, treating only the cake between the filter medium and slurry, and the pressure drop through the filter medium is very small compared to that through the cake. The boundary condition at the interface of the medium and cake is identical to that employed by other researchers [1,3,5,7,9].

Table 1. Boundary conditions of a filter cake

	All other researchers including Tiller and Shirato	Yim [10]
Medium-Cake interface	$x=0,\ p_l=0,\ p_s=\Delta p$	$x=0,\ p_l=0,\ p_s=\Delta p$
Slurry-Cake interface	$x=L,\ p_l=\Delta p,\ p_s=0$	$x=L,\ p_l\cong\Delta p,\ p_s=p_1$

However, at the interface of the suspension and cake, we use our own boundary condition. Other researchers have assumed that the solid compressive pressure at the 'slurry-cake' is zero. The authors Yim et al. [10] assume a very small solid compressive pressure at the first solid layer of cake, named p_1. The values of p_1 are very small, i.e. from several pascals to hundreds of pascals during filtration. When filtration is performed with suspensions forming a normally compressible cake, p_1, having such small values does not influence the filtration results. However, filtration that leads to the formation of a very compressible cake is strongly influenced by a small value of p_1. This will be discussed later.

The authors analyzed that the solid compressive pressure at 'slurry-cake' p_1 may be composed of the weight of sediment that pushes the cake and also may be composed of the drag force of the liquid flowing through the first solid layer. The solid compressive pressure at the first solid layer p_1 is the most important concept for the 'unified theory on solid-liquid separation', proposed by the authors [11]. The theory unifies cake filtration, expression of cake, hindered sedimentation, centrifugal filtration, and cross-flow filtration [11].

With the existing boundary conditions, Eq. (8) can be changed as follows:

$$\mu\rho_s v_o L=\int_0^{\Delta p}\frac{dp_s}{\alpha(1-\varepsilon)} \tag{9}$$

But the boundary condition proposed by the authors in Table 1 gives

$$\mu\rho_s v_o L=\int_{p_1}^{\Delta p}\frac{dp_s}{\alpha(1-\varepsilon)} \tag{10}$$

When Eq. (9) is integrated from x=0 to a certain cake thickness x=x, i.e., to $p=p_s$, Eq. (11) is obtained.

$$\mu\rho_s v_o x=\int_0^{p_s}\frac{dp_s}{\alpha(1-\varepsilon)} \tag{11}$$

Dividing Eq. (11) by (9), we obtain Eq. (12).

$$\frac{x}{L}=\frac{\int_0^{p_s}\frac{dp_s}{\alpha(1-\varepsilon)}}{\int_0^{\Delta p}\frac{dp_s}{\alpha(1-\varepsilon)}} \tag{12}$$

The average cake resistance of a very compressible cake calculated by the existing boundary conditions always gives negative values, and a negative average cake resistance cannot be accepted in cake filtration [10]. This subject is discussed in further detail later.

The boundary condition proposed by the author gives Eq. (13). There is no difference between this and Eq. (12) except that the initiation of integration begins at p_1 instead of zero. By this boundary condition, the average specific cake resistance is not negative [10].

$$\frac{x}{L}=\frac{\int_{p_1}^{p_s}\frac{dp_s}{\alpha(1-\varepsilon)}}{\int_{p_1}^{\Delta p}\frac{dp_s}{\alpha(1-\varepsilon)}} \tag{13}$$

By integrating Eq. (13), the relation between the solid compressive pressure p_s at any cake thickness x can be determined and, furthermore, the porosity at the cake thickness can also be calculated by using p_s. Finally, the porosity distribution in a cake can be verified.

1-2. Constitutive Equation of Cake

To integrate Eq. (12), the relations between either α and p_s or $(1-\varepsilon)$ and p_s must be established. Tiller [12] proposed the relations given below. The equations of this nature represent the fundamental characteristics of the cake, and are usually referred to as constitutive equations.

$$p_s>p_i \quad \alpha=ap_s^n \quad (1-\varepsilon)=Bp_s^\beta \tag{14}$$

$$p_s<p_i \quad \alpha=ap_i^n \quad (1-\varepsilon)=Bp_i^\beta \tag{15}$$

The values a, n, B, β in these equations express cake characteristics, and can be determined by a compression-permeability cell (CPC) test. In the CPC test, the solid compressive pressure p_s is applied directly on the cake surface. The specific cake resistance α and porosity ε at a certain value of p_s can be measured. When the measured values are arranged in log-log scale, straight lines are usually obtained and the values of a, n, B, β can be determined.

Among the above 4 properties, 'n', referred to as compressibility, is especially important. The compressibility of a cake does not mean the degree of physical compression, but rather a constant determined by Eq. (14) that shows the relation between p_s and α. In this study, a highly compressible cake signifies a cake having a value of n greater than unity.

Tiller [12] insisted that the value p_i in Eq. (15) also describes the cake characteristic, and can be determined in a CPC. His CPC results showed that α and ε did not vary when p_s is less than 1 kPa [12]. In his case, p_i is 1 kPa. This means that the porosity and specific cake resistance of a cake do not change at low solid compressive pressures. For a very compressible cake, this concept plays an important role in integrating Eq. (12).

Shirato et al. [13], however, showed that the porosity ε decreased until p_s was 100 Pa with particulate sediment, and Yim et al. [10] proved that ε decreased until p_s was 0.88 Pa, using floc sediment. Yim et al. [10] suggested the following very simple constitutive equations.

$$0<p_s \quad a=p_s^n \quad (1-\varepsilon)=Bp_s^\beta \tag{16}$$

When using Eq. (16), the boundary conditions given in Eq. (13) are essential.

The cake characteristics of bentonite floc, which is the object material of the present study, flocculated by anionic polymer flocculant and measured by CPC, are presented in Table 2.

1-3. Integration Results of Porosity Equation and Analysis

Eq. (17) is obtained by introducing Eqs. (14) and (15) into Eq. (12) with the existing boundary conditions.

$$\frac{x}{L}=\frac{\int_0^{p_s}\frac{dp_s}{\alpha(1-\varepsilon)}}{\int_0^{\Delta p}\frac{dp_s}{\alpha(1-\varepsilon)}}=\frac{\int_0^{p_s}\frac{dp_s}{ap_s^nBp_s^\beta}}{\int_0^{\Delta p}\frac{dp_s}{ap_s^nBp_s^\beta}}=\frac{\frac{1}{aB}\int_0^{p_s}\frac{dp_s}{p_s^{n+\beta}}}{\frac{1}{aB}\int_0^{\Delta p}\frac{dp_s}{p_s^{n+\beta}}} \tag{17}$$

Table 2. The characteristic values of the bentonite floc

$a=2.87\times10^7$	$n=1.125$
$B=4.09\times10^{-3}$	$\beta=0.317$

By Tiller's conception, Eq. (14) is composed of two regions: from 0 to p_i and from p_i to Δp. When these regions are applied, we obtain:

$$\frac{x}{L}=\frac{\int_0^{p_i}p_i^{-(n+\beta)}dp_s+\int_{p_i}^{p_s}p_s^{-(n+\beta)}dp_s}{\int_0^{p_i}p_i^{-(n+\beta)}dp_s+\int_{p_i}^{\Delta p}p_s^{-(n+\beta)}dp_s}=\frac{p_i^{(1-n-\beta)}+\frac{p_s^{(1-n-\beta)}-p_i^{(1-n-\beta)}}{1-n-\beta}}{p_i^{(1-n-\beta)}+\frac{\Delta p^{(1-n-\beta)}-p_i^{(1-n-\beta)}}{1-n-\beta}} \tag{18}$$

Arranging this equation, Eq. (19) is obtained.

$$\frac{x}{L}=\frac{p_s^{(1-n-\beta)}-(n+\beta)p_i^{(1-n-\beta)}}{\Delta p^{(1-n-\beta)}-(n+\beta)p_i^{(1-n-\beta)}} \tag{19}$$

Identical procedures can be performed with the author's Eqs. (13) and (16). Then,

$$\frac{x}{L}=\frac{\int_{p_1}^{p_s}\frac{dp_s}{\alpha(1-\varepsilon)}}{\int_{p_1}^{\Delta p}\frac{dp_s}{\alpha(1-\varepsilon)}}=\frac{\int_{p_1}^{p_s}\frac{dp_s}{ap_s^nBp_s^\beta}}{\int_{p_1}^{\Delta p}\frac{dp_s}{ap_s^nBp_s^\beta}}=\frac{p_s^{(1-n-\beta)}-p_1^{(1-n-\beta)}}{\Delta p^{(1-n-\beta)}-p_1^{(1-n-\beta)}} \tag{20}$$

During filtration p_i at Eq. (19) is less than 1,000 Pa, and the value is much smaller than the ordinary filtration pressure Δp. p_1 from Eq. (20) is also very small, i.e., less than 100 Pa. For the filtration of a suspension composed of particles, not of flocs, the value of $(n+\beta)$ is less than unity, normally less than 0.4. As a result, either the value of $\Delta p^{(1-n-\beta)}$ or $p_s^{(1-n-\beta)}$ is much greater than that of $(n+\beta)p_i^{(1-n-\beta)}$. The term $(n+\beta)p_i^{(1-n-\beta)}$ can be ignored in Eq. (16). For the same reason, the term $p_1^{(1-n-\beta)}$ in Eq. (20) can also be omitted. For the filtration of floc, which forms a highly compressible cake, the value of $(n+\beta)$ is greater than unity. Either the value of $\Delta p^{(1-n-\beta)}$ or $p_s^{(1-n-\beta)}$ is much smaller than that of $(n+\beta)p_i^{(1-n-\beta)}$ or $p_1^{(1-n-\beta)}$. In this study, we deal with these cases. The role of p_i of p_1 is very important in this case.

2. Regarding the Definition of Dense Skin

The porosity distribution calculated by Tiller and Lew [3] is shown on Fig. 1. The location where x/L is zero indicates the interface of the filter medium and cake, and that where x/L is 1 denotes the in-

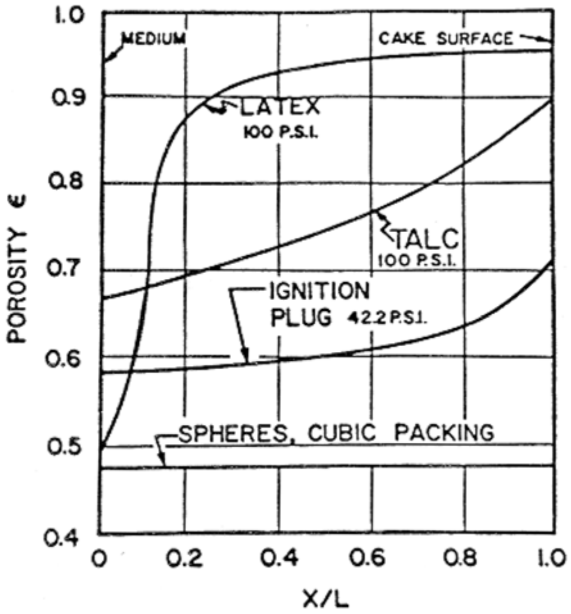

Fig. 1. Porosity distributions for materials with various compressibilities (Tiller and Leu [3]).

terface of the suspension and cake.

The lower horizontal line is the porosity distribution of an incompressible material; the porosity in the cake is uniform. The ignition floc in the figure has a compressibility n of roughly 0.4. Only a small extent of porosity change occurs between the interface of the medium-cake to about 2/3 of the total cake thickness. At the vicinity of the interface of the suspension-cake, the porosity changes considerably. This ignition floc line represents the porosity distribution of a normally compressible cake. Shirato et al. [5] obtained this porosity distribution curve via an indirect method by measuring liquid pressures at various depths in the filter cake.

The porosity distribution of latex in Fig. 1 represents highly compressible cakes. The compressibility n of the latex is about 3. In contrast to the porosity distribution of the ignition floc, the porosity variation at the vicinity of the medium is very great and almost all the variation takes place at this region. After this region, the remainder of the cake has a porosity greater than 0.9, i.e., the cake has high water content and thus arguably it can hardly be described as a solid bed of particles.

This type of porosity distribution has never been measured but only calculated. Our goal then is to experimentally measure the porosity distribution of a cake formed with a highly compressible material.

Thus far, we have employed the expression ‘dense skin’. The so called ‘dense skin’ refers to the region near the medium for the porosity distribution of latex shown in Fig. 1. However, it is difficult to clearly define the limit of dense skin in the cake shown in Fig. 1. In this study, we adopt the definition of Tiller and Green [2] for dense skin: “a thin skin of dry, resistant material next to the media during filtration.”

3. Influence of Filtration Pressure on Flow Rate

Eq. (1) can be changed as follows for calculating the flow rate according to the filtration pressure.

$$v_o \mu dW = \frac{dp_l}{\alpha} \tag{21}$$

As α is a function of pressure, Eq. (21) can be changed into Eq. (22).

$$v_o \mu \int_0^W dW = \int_{p_1}^{\Delta p} \frac{dp_l}{\alpha} \tag{22}$$

In Eq. (22), Yim’s boundary conditions are applied. For Tiller’s boundary conditions, p_1 will be changed to 0; this means that α has a constant value between a pressure of 0 and p_i and α varies according to the constitutive equation from p_i to Δp as given by Eqs. (14) and (15). When appropriate values are adopted for p_1 and p_i, the values of the average specific cake resistance are identical; therefore, we continue with Eq. (22).

Integrating Eq. (22), we can obtain

$$v_o \mu W = \int_{p_1}^{\Delta p} \frac{dp_l}{a p_s^n} = \frac{\Delta p^{(1-n)} p_1^{(1-n)}}{a(1-n)} \tag{23}$$

The cake characteristics a and n in Eq. (23) are shown in Table 2. The value of p_1 changes slightly according to the filtration conditions; we use a value of 2.5 Pa, which was obtained in filtration experiments. The filtrate viscosity μ is 0.001 kg/m·s. We take the cake mass per unit filtration area W as 3.2 kg/m^2 for which the experimental procedures were performed.

With these values, the flow rate v_o can be calculated at various filtration pressures, Δp.

4. Methods for Determining Porosity Distribution in a Cake

Several methods have been proposed for determining the porosity distribution in a cake. In 1953, Rietema [4] measured the electrical conductivity between pins situated at the same height at opposite sides of a filtration cell. Several pins were arranged in the cell from the bottom to the top of cake at equal intervals. Lower porosity of the cake was found to give smaller conductivity. The porosity distribution was obtained on the basis of the relation between the electrical conductivity and porosity.

In 1971, Shirato et al. [5] improved the above experimental apparatus. Instead of pins, they used thin disks of 3 mm diameter and 1 mm thickness. The disks were installed inside the filtration cell, and thus the formation of cake was not hindered by the discs. In Rietema’s experiment [4], the point of the pin disturbed the formation of a uniform cake in the horizontal direction, and it was almost impossible to make the pin points having the same conduction area. Shirato et al. [5] corrected these defects, but the 3 mm disks were too wide to measure the existence of dense skin, which may be thinner than the width of the disk. Thus far, no experimental results using these methods have been reported to verify the existence of the dense skin.

Okamura and Shirato [6] measured the distribution of liquid pressure in cake during filtration at heights of 0.25 cm, 0.44 cm, 0.74 cm, 1.05 cm, 1.36 cm, and 1.65 cm from the filter medium using 6 tubes of 3.5 mm inside diameter. The measured liquid pressures were converted into solid compressible pressures using Eq. (2), and the porosities at the positions were then obtained with Eq. (14). They used a suspension composed of particles, and thus the cake was normally formed below the 3.5 mm tube. In our preliminary study, this method was applied. For the filtration of floc, which forms a highly compressible material, cake is not formed below the 3.5 mm tube, but rather this region is filled with water. The pressure drop was not measured, and thus the method was not appropriate for proving the existence of dense skin.

In 1957, Hutto [7] made thin colored bands in a cake by adding a suspension composed of colored particles. He changed the flow of normal suspension and colored particle suspension into the cell by opening and shutting the inlet valves. After a certain amount of the normal filtration, the supply line was shut, and a small amount of the suspension of colored particles was introduced into the filtration cell. These operations were performed alternately. At lower porosity, a slice of cake distinguished by colored bands had thinner thickness, and vice versa. The porosity can be calculated according to the slice thickness.

For floc filtration, which forms a highly compressible cake, the dense skin can be terminated in the first slice. The coloring of the floc, however, may change the characteristics of the floc and floc-formed cake. We concluded this experimental method is not adequate to determine the dense skin. For the above reasons, we developed a new apparatus described in the following section.

EXPERIMENTAL

1. Filtration Apparatus for Measuring Distribution of Poros-

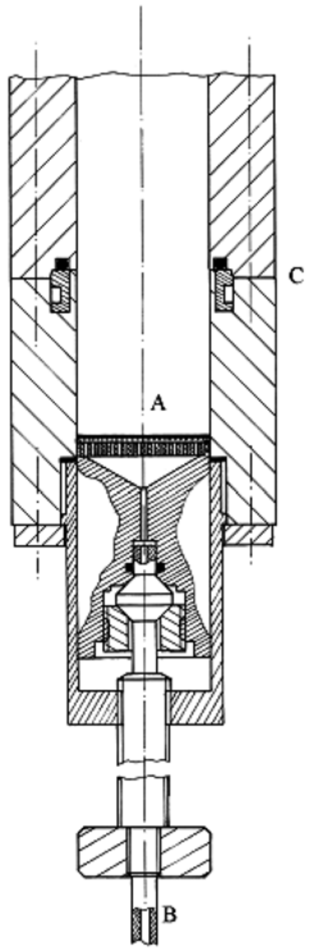

Fig. 2. Filter cell for slicing cake.

ity in Cake

The filtration apparatus for measuring the distribution of porosity in the cake is shown on Fig. 2. The inside diameter of the cell is 4 cm, and filtration proceeds in the cell filled with sedimented floc. Filtrate flows through the filter medium, which is designated by a thick horizontal line below the letter 'A' in Fig. 2. The filtrate then gathers at the funnel-shaped space, and flows through the narrow tube at the center until it reaches position 'B'. At the beginning of filtration, all of the cell is filled with sedimented floc. The sedimented floc is not cake. While filtration proceeds, the sedimented floc changes into cake. However, the boundary between the sedimented floc and cake is not visible or detectable. At the end of filtration, all of the sediment has changed into cake. The method employed for determining the ending of filtration will be discussed later.

Formation of filter cake starts on the filter medium, which is under position 'A'. At the end of filtration, the cake height reaches near position 'C'.

To separate and slice the formed cake, the cell was designed to be divided into two parts. When the upper part above position 'C' is detached, the lower part having cake remains.

When the larger part above 'B', designated by sparse diagonal lines, is rotated one round, the filter medium and support ascend 1 mm with the cake. The cake does not rotate and only ascends. Fig. 2 shows the state after ascending several millimeters along the filter medium and support. The excess portion of the filter medium cut by ascending support is shown on the figure as a short thick black line.

At first the portion of cake above 'C' is cut clearly, then the larger part above 'B' is turned one round to ascend the cake by 1 mm. The mounted 1 mm cake is cut and transferred to paper that was previously dried and weighed in the balance. To cut the slice precisely, a metal frame was installed around the cell wall at position 'C', which is designated with dense diagonal lines.

In this experiment it is critical not to leave any cake on the filter medium when the last slice has been cut. This problem was solved through several preliminary experiments.

This apparatus was manufactured by an expert technician who had extensive experience making rocket nozzles.

2. Experimental Material and Flocculant

The material used in our investigation is chemical floc flocculated with a bentonite suspension by an anionic polymer flocculant (Cyanamid Superfloc C 581). Flocculation was performed in an ordinary jar tester with 1 min rapid mixing at 130 rpm followed by 15 min slow mixing at 60 rpm. After flocculation, sedimentation was allowed to proceed for 10 min and the supernatant was then carefully eliminated. With the sedimented floc, filtration could be started.

Different from biological flocs, the chemical floc fabricated by the aforementioned procedure always has the same filtering characteristics. Furthermore, the cake formed by chemical floc has a compressibility value of 1.125, which reflects a highly compressible cake.

RESULTS AND DISCUSSION

1. Results of Filtration-Permeation

The results of the filtration-permeation experiment with bentonite floc using the apparatus shown in Fig. 2 are presented in Fig. 3. In a filtration-permeation approach developed by the authors [14], an ordinary filtration procedure is performed and then permeation of particle eliminated water through the pre-formed cake is successively followed.

In the ordinary filtration procedure of sedimented floc, it is not possible to distinguish the formed cake from the floc. Moreover, the expression of cake begins at the end of filtration, and there is no detectable difference between the end of filtration and the beginning of expression. The total height of the floc and cake, respec-

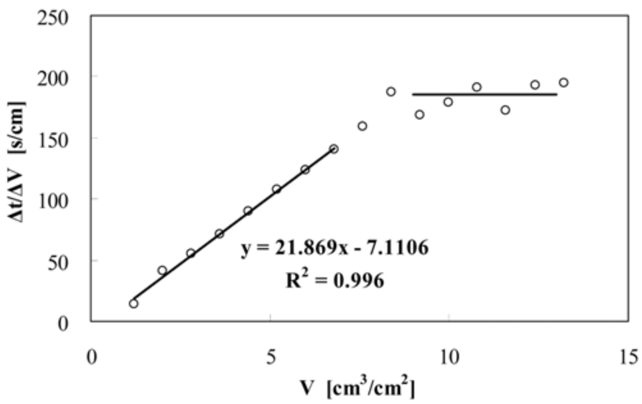

Fig. 3. Filtration-permeation results of bentonite floc at 0.5 atm.

tively, gradually decreases during filtration, and the height of the cake decreases during expression. Neither the end point of filtration nor the final filtration cake thickness could be determined. As the final filtration cake thickness cannot be determined, it is not possible to determine the total porosity distribution even if the porosities for a certain part of the cake are measured.

With filtration-permeation, the obtained cake does not include sediment or expressed cake. Without this method, the exact verification of the existence of 'dense skin' is very difficult.

In Fig. 3, the x-axis signifies filtrate volume per unit filtration area [cm^3/cm^2], and y-axis is the differential time per differential filtrate volume per unit filtration area [$s/(cm^3/cm^2)$]. The experimental results shown in Fig. 3 can be divided into two categories. The inclined straight line situated in the left side signifies the filtration period. With Ruth's equation, the average specific cake resistance is calculated as 3.13×10^{11} m/kg.

The horizontal line indicates the permeation period, during which all of the floc in the filter cell is transformed into cake. With the cake mass per unit filter area W, the average specific cake resistance can be calculated, yielding a value of 2.95×10^{11} m/kg.

In this case, the two average specific cake resistances measured by filtration and permeation are identical within the experimental error limits. When sedimentation occurs during filtration, the two values do not coincide.

The porosity distribution was measured for the cake after the end point shown in Fig. 3.

2. Porosity Distribution in Cake and Verification of Dense Skin

2-1. Experimental Results of Porosity Distribution

The porosity distribution of a cake, which was obtained by filtration-permeation as presented in Fig. 3, is shown in Table 3. The pressure for filtration-permeation was 0.5 atm. The porosity distribution was measured by the apparatus shown in Fig. 2.

The first row of Table 3 shows the weights of papers that were dried for 1 hour at 105 °C and cooled to the room temperature in a

Table 3. Experimental results of sliced cake formed by bentonite floc filtration at 0.5 atm

Paper mass [g]	Paper+cake [g]	Cake mass [g]	Porosity [-]	Cake height [mm]
0.127	0.249	0.122	0.983	2.20
0.129	0.249	0.120	0.983	2.00
0.127	0.255	0.128	0.982	1.80
0.129	0.264	0.135	0.981	1.60
0.127	0.268	0.141	0.980	1.40
0.129	0.283	0.154	0.979	1.20
0.128	0.211	0.083	0.977	1.05
0.128	0.214	0.086	0.976	0.95
0.130	0.222	0.092	0.974	0.85
0.128	0.225	0.097	0.973	0.75
0.128	0.232	0.104	0.971	0.65
0.128	0.243	0.115	0.968	0.55
0.128	0.256	0.128	0.964	0.45
0.129	0.276	0.147	0.959	0.35
0.130	0.310	0.180	0.950	0.25
0.127	0.355	0.228	0.936	0.15
0.128	0.477	0.349	0.903	0.50

desiccator before weighing. The difference in weight between individual pieces of weighing paper is a maximum of 3 mg.

Sliced cake of 1 mm or 2 mm thickness was transferred to the weighing paper. The sliced cake on the weighing paper was dried for 1 hr at 105 °C and then cooled in the desiccator before weighing. The total weight of the dried cake and weighing paper is shown in the second row of Table 3. The third row represents the dried cake mass, which has been calculated from the second and first rows. The fourth row shows the porosity of the sliced cake calculated by the particle density 2.85 g/cm^3, the filter area from the inside diameter of the cell, i.e., 4 cm, and the thickness of the sliced cake. The fifth row is the mean height from the filter medium to each slice of cake. The first line is the upper part of the cake, and the 17^{th} line shows the data of a 1 mm slice of the cake situated on the filter medium. The six sliced cake sections from the first line have 2 mm thickness, and the succeeding 11 sliced cake sections have 1 mm thickness. We can see that the lower part of the cake has more mass by the 4^{th} row, and has smaller porosity by the 5^{th} row.

2-2. Porosity Distribution of Cake: Experimental and Theoretical Values

In Fig. 4, the experimental results of paragraph 2-1, i.e., the porosity distribution of a cake formed by bentonite floc filtration, are shown with white points, and the theoretical results calculated by Eq. (20) are delineated by a thick line. In Eq. (20), our constitutive equation and boundary condition are applied.

For the calculation, the cake characteristics obtained from the CPC test and the value of p_1 needed for the unified theory are adopted. The value of p_1 suitable for the graph was 1.0 Pa.

The porosity distributions of the cake formed at filtration of 2 atm, obtained by the same experimental method and theory, are shown in Fig. 5. The cake was divided into 16 slices from the filter medium, and the porosities were measured. The value of p_1 for the calculation is also 1.0 Pa. The shapes of the results from 0.5 atm and 2 atm are similar. The results of a cake formed under 1 atm were also measured. This shows the same shape, but is not discussed in this study.

At the vicinity of the filter medium (x/L=0), the existence of a thin area having lower porosity can be verified in Figs. 4 and 5. The thin area characterized by low porosity and a sudden porosity change can be called a dense skin. Thus, the existence of dense skin is experimentally verified for the first time.

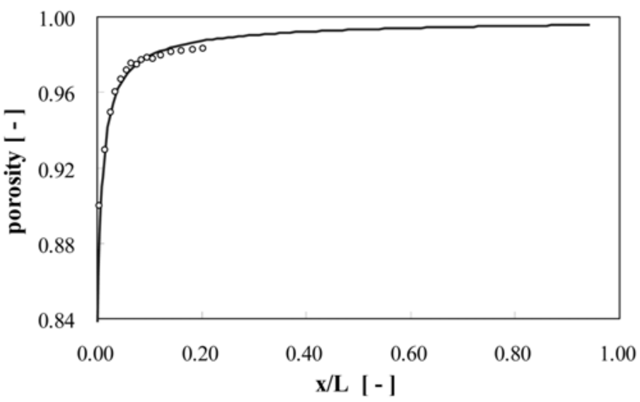

Fig. 4. Porosity distribution in a cake formed by bentonite floc at 0.5 atm.

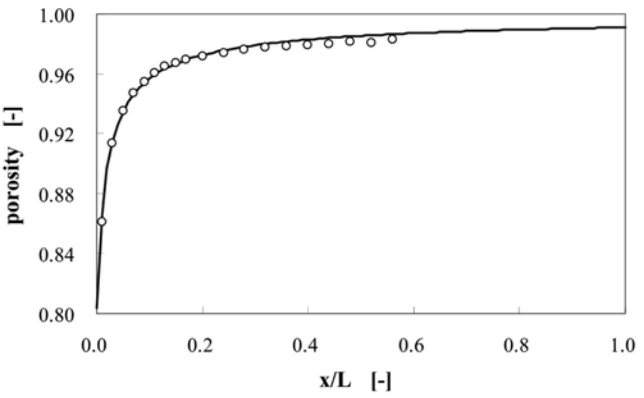

Fig. 5. Porosity distribution in a cake formed by bentonite floc at 2 atm.

The coincidence between experimental results and theoretical results signifies the following. First, the porosity and specific cake resistance change until a very small solid compressible pressure, as given by Eq. (16). This is proposed by the author. Second, the new boundary condition p_1 proposed by the author [10] shown in Table 1 is appropriate for calculating the porosity distribution.

In Figs. 4 and 5, the theoretical porosities are larger than the experimental porosities when x/L is greater than 0.1. The porosities of the region are greater than 0.98, indicating that the properties of the cake at this region are similar to those of floc sediment. Other researchers do not consider this region to be cake. By the experimental results of filtration-permeation shown on Fig. 3, we concluded that this region is cake. To measure the porosity of this high porosity region, the cake was pushed towards position 'C' in Fig. 2. By this pushing operation, the fragile cake could be somewhat compressed. It is reasonable that the compression is not observed at cake having low porosity. Thus experimental and theoretical results coincide at dense skin.

2-3. Porosity Distribution at the Vicinity of the Filter Medium

The porosity distribution near the filter medium, x/L, is zero to 0.04 (Fig. 6). Theoretical calculations at 0.125 and 8 atm are added to the experimental and theoretical results for 0.5 atm and 2 atm.

The upper bold line and small white squares represent the experimental and theoretical porosity distribution at 0.5 atm, respectively, and the lower bold line and white circlets are those at 2 atm.

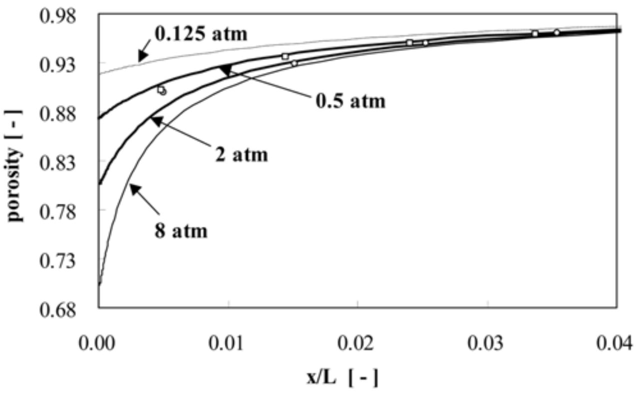

Fig. 6. Porosity distribution in a cake at the vicinity of the filter medium at various filtration pressures.

Table 4. Calculated porosity at the vicinity of the filter medium and 4% depth

Δp (atm)	Porosity (ε) at x/L=0.0001	Porosity (ε) at x/L=0.04
0.125	0.919	0.967
0.5	0.874	0.964
2	0.806	0.962
8	0.703	0.961

The deviation of the first circlet originates from difficulty in exactly cutting the first slice from the filter medium. However, the deviation is not large enough to be detected in Fig. 5, which shows the total thickness range.

From the second set of data, experimental and theoretical results coincide well, as shown in Fig. 6; at x/L is nearly 0.03, and almost all the theoretical results of various pressures from 0.125 to 8 atm are too close to be verified by the experiment. With the theoretical study, it can be concluded that the porosity difference in a cake caused by filtration pressure is limited only at the vicinity of the filter medium.

To verify this, we calculated the porosity at x/L of 0.001 and 0.04. The results are shown in Table 4. The porosity at x/L varies considerably with the filtration pressure. However, at x/L=0.04, the difference in the porosities falls within the experimental error limits. We can conclude that the porosities of the remaining 96% thickness are very similar for various filtration pressures. As most of the cake has identical porosity, the average porosity of the cake may not be influenced by variation of the lower 4% thickness.

Owing to the peculiar properties originating from dense skin, high pressure for filtration cannot contribute to reducing the average porosity for highly compressible cake filtration [3].

3. Variation of Filtrate Flow Rate According to Filtration Pressure

The rate of filtrate v_o of a highly compressible cake at various filtration pressures using Eq. (23) is shown in Table 5. Eq. (23) adopts the boundary condition proposed by the author.

When the filtration pressure increases fivefold, i.e., from 0.1 atm to 0.5 atm, the filtrate flow rate v_o increases only 10%, from 5.01×10^{-5} m/s to 5.52×10^{-5} m/s. An increase of pressure from 1 atm to 5 atm also provides only a 7% increase in the filtrate flow rate. The filtration pressure does not influence the flow rate for a highly compressible cake.

For comparing the phenomenon with a moderately compressible

Table 5. Filtrate flow rate of a very compressible cake (n=1.125) at various filtration pressures

Δp (atm)	v_o (m/s)	$\Delta p^{(1-n)}$	$p_1^{(1-n)}$
0.01	4.09E-05	0.422	0.892
0.05	4.76E-05	0.345	0.892
0.1	5.01E-05	0.316	0.892
0.5	5.52E-05	0.259	0.892
1	5.70E-05	0.237	0.892
5	6.08E-05	0.194	0.892
10	6.22E-05	0.178	0.892

Table 6. Filtrate flow rate of a very compressible cake (n=0.3) at various filtration pressures

Δp (atm)	v_o (m/s)	$\Delta p^{(1-n)}$	$p_1^{(1-n)}$
0.01	2.24E-06	126	1.899
0.05	6.99E-06	388	1.899
0.1	1.14E-05	631	1.899
0.5	3.51E-05	1,947	1.899
1	5.71E-05	3,162	1.899
5	1.76E-04	9,756	1.899
10	2.86E-04	15,849	1.899

cake (n=0.3), identical calculations were performed and are shown in Table 6. The value of 'a' was set to have the same at 1 atm.

In Table 6, a fivefold increase of filtration pressure, from 0.1 atm to 0.5 atm, gives a 208% increase of the filtrate flow rate v_o, from 1.14×10^{-5} m/s to 3.51×10^{-5} m/s. The case of a pressure increase from 1 atm to 5 atm also gives a 208% increase of v_o. Although v_o does not increase by five time for a fivefold increase of pressure, the tendency is very different from that of the highly compressible cake.

In Table 5, a highly compressible cake has a large value of $p_1^{(1-n)}$ compared to $\Delta p^{(1-n)}$ at all filtration pressures. In the right hand side of Eq. (23), the numerator is more strongly influenced by the constant $p_1^{(1-n)}$ than by $\Delta p^{(1-n)}$. Therefore, the influence of the filtration pressure Δp on the flow rate is small. The flow rate depends on the constant $p_1^{(1-n)}$. For this reason, the filtrate flow rate has almost the same value at various pressures.

For filtration with a moderately compressible cake, as shown in Table 6, the value of $p_1^{(1-n)}$ is remarkably smaller than that of $\Delta p^{(1-n)}$, and thus the term $p_1^{(1-n)}$ can be eliminated for filtrations proceeding at pressure higher than 0.5 atm.

To effectuate fast filtration, it is normal procedure to perform filtration at high pressure for a moderately compressible cake, as shown in Table 6. For a highly compressible cake, high pressure increases the flow rate to a very small extent. High pressure decreases only the porosity of dense skin, as shown in Fig. 6, and the dense skin decreases the flow rate.

CONCLUSION

Using a new experimental apparatus developed in this study, we measured the porosity distribution in a highly compressible cake. The existence of 'dense skin' was thus verified experimentally. The theoretical porosity distribution was calculated with a new constitutive equation and a new boundary condition of cake by using a 'unified theory of solid-liquid separation'. The experimental porosity distribution coincides with the theoretical calculations. The characteristics of dense skin were analyzed by experimental and theoretical means, and the influence of dense skin on the average cake porosity and filtration rate was investigated.

ACKNOWLEDGMENT

This work was supported by an INHA UNIVERSITY Research Grant.

REFERENCES

1. P. C. Carman, *Transactions. - Institution of Chemical Engineers*, 168 (1938).
2. F. M. Tiller and T. C. Green, *AIChE J.,* **19**(6), 1266 (1973).
3. F. M. Tiller and W. Leu, World Filtration Congress III, 270 (1982).
4. K. Rietema, *Chem. Eng. Science*, **2**, 88 (1953).
5. M. Shirato, M. Aragaki, K. Ichimura and N. Ootsuji, *J. of Chem. Eng. of Japan*, **4**(2), 172 (1971).
6. S. Okamura and M. Shirato, *Kagaku Kogaku*, **19**(8), 104 (1955).
7. F. B. Jr. Hutto, *Chem. Eng. Progr.*, **53**(7), 328 (1957).
8. F. M. Tiller and H. Cooper, *AIChE J.*, **8**(4), 445 (1962).
9. H. P. G. Darcy, *Victor delmont*, Paris (1856).
10. S. S. Yim, Y. M. Song and Y. D. Kwon, *Korean J. Chem. Eng.*, **20**, 334 (2003).
11. S. S. Yim, 7th World Filtration Congress, Budapest, Hungary, 127 (1996).
12. F. M. Tiller, *Chemical Engineering Progress*, **51**(6), 282 (1955).
13. M. Shirato, T. Murase, E. Iritani and N. Hayashi, *Filtration and Separation*, Sept/Oct, 404 (1983).
14. S. S. Yim and R. Ben Aim, 4th World Filtration Congress, June, Ostend Belgium (1986).
15. S. S. Yim, Y. M. Song and J. Y. Lee, *HWAHAK KONGHAK*, **41**(4), 471 (2003).